*D. L. McDiarmid**

The Effect of Mean Stress on Biaxial Fatigue where the Stresses are Out-of-Phase and at Different Frequencies

REFERENCE McDiarmid, D. L., **The effect of mean stress on biaxial fatigue where the stresses are out-of-phase and at different frequencies**, *Biaxial and Multiaxial Fatigue*, EGF 3 (Edited by M. W. Brown and K. J. Miller), 1989, Mechanical Engineering Publications, London, pp. 605–619.

ABSTRACT The results of tests on thin wall cylinders subjected to biaxial stresses are reported, and include mean stress effects, and stresses which are out-of-phase and at different frequencies. It is suggested that the maximum shear stress criterion of failure, modified for the effects of mean and alternating normal stresses acting on the plane of maximum range of shear stress, is a reasonable basis for long life fatigue predictions under such complex stress situations.

Introduction

It has long been recognised that many components in service are subject to complex multiaxial fatigue stress conditions. These include axles, crank shafts, and propellor shafts subjected to combined bending and twisting which can be out-of-phase and at different frequencies. Pressure vessels and piping are other examples, and many notches and geometric discontinuities are subject to such complex stress situations. Due to the difficulty and expense of attempting to conduct meaningful tests under such a variety of complex stress situations many attempts have been made to derive theories which can cope with these complex multiaxial fatigue stress situations based on simple laboratory test data such as the uniaxial reversed stress fatigue test. A considerable number of theories of multiaxial fatigue have been proposed and many are reviewed in references (**1**) and (**2**).

The author has, amongst others, proposed (**3**)(**4**) that the important parameters for long life fatigue in the unnotched situation are the alternating and mean stresses, both normal and shear, occurring on the plane of maximum range of shear stress. This theory has been extended for the case of out-of-phase biaxial stresses (**5**)(**6**), where it is shown that the out-of-phase stresses produce shorter fatigue lives than equal in-phase stresses. A further extension of this work (**7**) has been carried out for the case where the biaxial stresses are not only out-of-phase but also at different frequencies.

The present paper describes the results of further tests conducted under similar conditions to those in (**7**) in an attempt to consolidate the tentative

* Department of Mechnical Engineering, The City University, London, UK.

conclusions of the earlier work. Further tests have also been conducted to extend the investigation of the out-of-phase cases to include the effect of mean stress. These test cases allow the separate effects to be studied of alternating and mean stresses, both normal and shear, on the plane of maximum range of shear stress.

Notation

b	Fatigue limit under reversed bending
t	Fatigue limit under reversed torsion
α	Frequency ratio = frequency of σ_{2a}/frequency of σ_{1a}
λ	Principal stress amplitude ratio = σ_{2a}/σ_{1a}
φ	Out of phase angle, where σ_2 leads σ_1; related to σ_2 where 1 cycle of σ_2 if 360 degrees
$\sigma_1, \sigma_2, \sigma_3$	Principal stresses ($\sigma_1 > \sigma_2 > \sigma_3$)
$\sigma_{1a}, \sigma_{2a}, \sigma_{3a}$	Principal stress amplitudes
σ_a	Stress amplitude
σ_A	Uniaxial reversed fatigue strength
σ_m	Mean stress
σ_n	Normal stress amplitude on the plane of maximum range of shear stress
σ_{nm}	Mean normal stress on the plane of maximum range of shear stress
σ_T	Tensile strength
$\sigma_{n12}, \sigma_{n23}, \sigma_{n23}$	Normal stress amplitudes in the 12, 23, 31 planes of maximum range of shear stress
τ	Shear stress amplitude
$\tau_{12}, \tau_{23}, \tau_{31}$	Shear stress amplitudes on the 12, 23, 31 planes of maximum range of shear stress
τ_a	Shear stress amplitude on the plane of maximum range of shear stress
τ_m	Mean shear stress on plane of maximum range of shear stress
12, 23, 31	Planes of maximum range of shear stress associated with the *1*, *2*, *3* principal stress directions
1, 2, 3	Longitudinal, transverse, and radial directions, respectively

Experimental program

Three series of fatigue tests were carried out on thin wall tubular specimens. In the first series specimens were subjected simultaneously to constant amplitude alternating longitudinal load and alternating differential pressure across the wall thickness. These tests covered the same range of principal stress amplitude ratio, out-of-phase, and frequency ratio as used in (7) and shown in Table 1.

The second series of tests were conducted to determine the effect of mean stress under longitudinal stress only and transverse stress only.

Table 1 Test conditions for Series 1. For all tests, σ_1 is the longitudinal and σ_2 is the transverse stress

Case	$\lambda = \frac{\sigma_{2a}}{\sigma_{1a}}$	φ = *Phase angle (degrees)*	$\alpha = \frac{\textit{Frequency of } \sigma_{2a} \text{ (=30 Hz)}}{\textit{Frequency of } \sigma_{1a}}$
1	0		
2	∞		
3	1	0	1
4	1	180	1
5	1	0	2
6	1	90	2
7	1	0	3
8	1	180	3

The third series of tests were conducted at an amplitude ratio of unity and out-of-phase angle of 180 degrees with various combinations of mean and alternating stress, both longitudinal and transverse, as detailed later.

Note that in the testing $\sigma_1 = \sigma_{\text{longitudinal}}$ and $\sigma_2 = \sigma_{\text{transverse}}$ stresses. The frequency of σ_{2a} was the greater, and equalled 30 Hz in the tests reported here.

Material and specimens

The material used in this investigation was EN 24 T steel. The nominal material chemical composition is detailed in reference (7). The minimum specification mechanical properties were:

tensile strength	850 MN/m^2
yield stress	680 MN/m^2
elongation	18 per cent

The specimen dimensions are shown in Fig. 1.

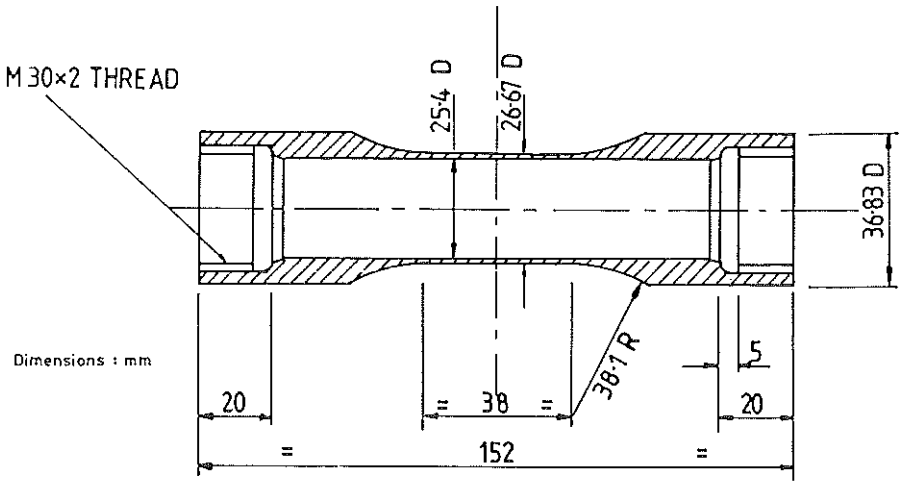

Fig 1 Specimen geometry and dimensions

The specimens used in this investigation were from a new batch of material and were produced by a different manufacturer compared to those used previously (7). The outside diameter was again produced with a fine tapered finish, but the final finish of the bore was obtained here by honing rather than by the use of a special reamer as in (7).

Test equipment

The thin wall tubular specimen was mounted in a pressure test cell device, shown in Fig. 2, capable of producing a differential pressure across the wall

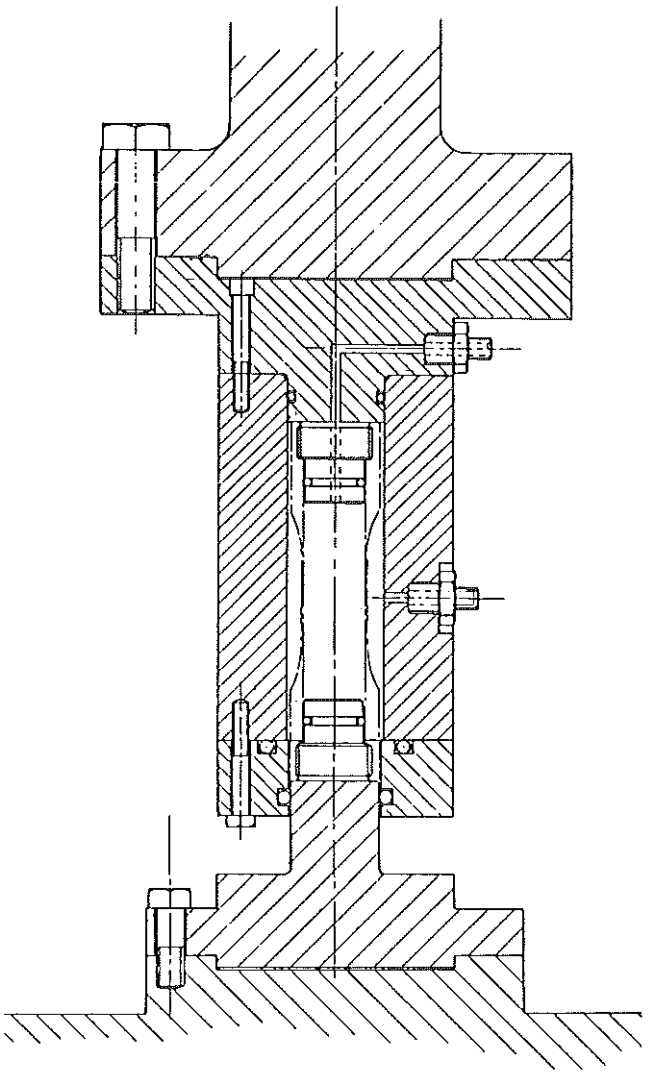

Fig 2 The pressure test cell

thickness. The facility was then assembled in a standard 250 kN Schenck fatigue test machine. The complete test system is described in (7). It is relevant to note that the bore and annular areas of the specimen subject to pressure were arranged to be equal. Hence, a constant tensile longitudinal stress (regardless of the value of the differential pressure applied across the wall thickness) due to the pressure, acted on the thin wall section of the specimen, but this could be offset if required, by an actuator load to obtain only an alternating differential pressure with no longitudinal stress.

Test results and discussion

Series one tests

The results of the series one tests are shown in Fig. 3. The material is seen to be anisotropic, the transverse fatigue strength being about 80 per cent of the longitudinal fatigue strength compared with 60 per cent in (7). These results are compared in Fig. 4 with those found under the same test conditions in (7). *S–N* curves for test cases 1–8 are shown in Fig. 4 and can be compared with the corresponding curves from (7) in Fig. 5.

It is seen that the uniaxial longitudinal reversed stress fatigue strength of the current material is lower than that of the material used in (7), and also that the degree of anisotropy with regard to the corresponding transverse fatigue strength is less. These properties are compared in Table 2 along with tensile test data.

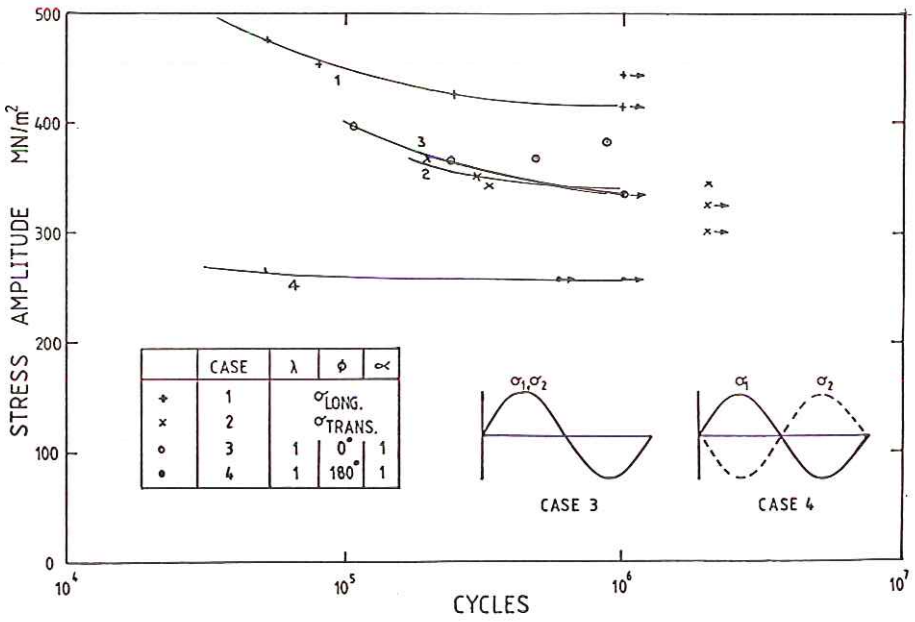

Fig 3(a) Test results – cases 1–4

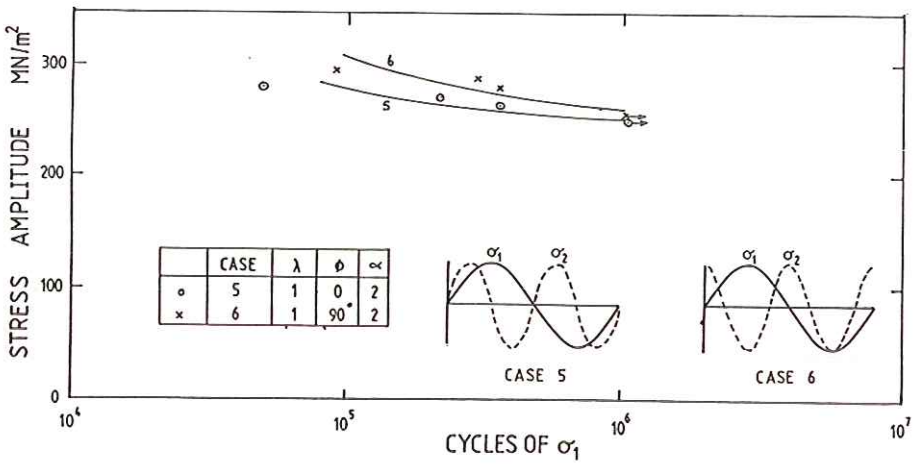

Fig 3(b) Test results – cases 5 and 6

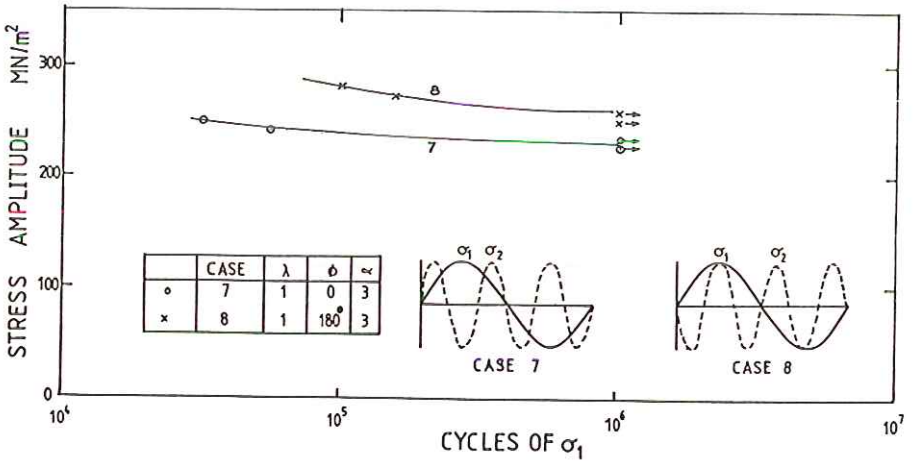

Fig 3(c) Test results – cases 7 and 8

Table 2 Fatigue and tensile strengths

	Current work	*Reference* (7)
Tensile strength (MN/m²)	993	974
Longitudinal fatigue strength (10^6 cycles) (MN/m²)	420	470
Transverse fatigue strength (10^6 cycles) (MN/m²)	340	270

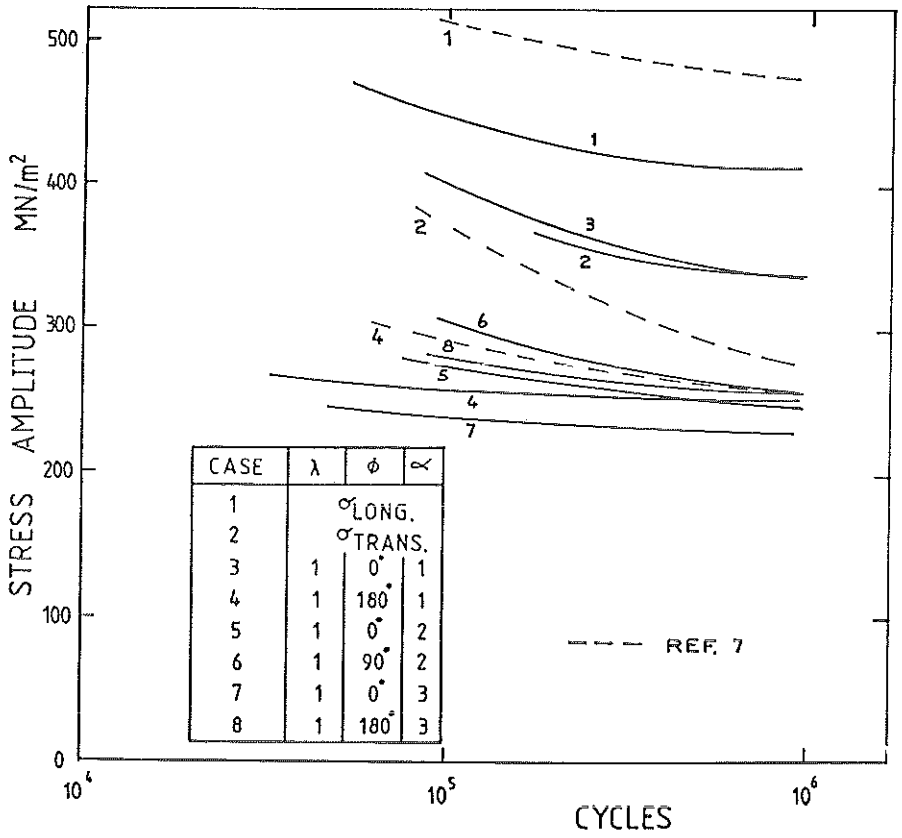

Fig 4 Test results – cases 1–8

Table 3 Predicted and experimental fatigue limit (10^6 cycles) strengths

Case	$\frac{\tau_{12}}{\sigma_{1a}}$	$\frac{\tau_{23}}{\sigma_{1a}}$	$\frac{\tau_{31}}{\sigma_{1a}}$	σ_{1a}/σ_A *Predicted*	σ_{1a}/σ_A *Experimental*
1	*0.5*	0	*0.5*	1	(1)
2	0.5	*0.5*	0		0.82 (0.60)
3	0	*0.5*	0.5		0.82 (0.60)
4	*1.0*	0.5	0.5	0.5	0.63 (0.56)
5	*0.88*	0.5	0.5	0.57	0.61 (0.62)
6	*0.8*	0.5	0.5	0.63	0.63 (0.63)
7	*1.0*	0.5	0.5	0.5	0.57 (0.58)
8	*0.85*	0.5	0.5	0.59	0.63 (0.62)

Figures in brackets from reference (7).

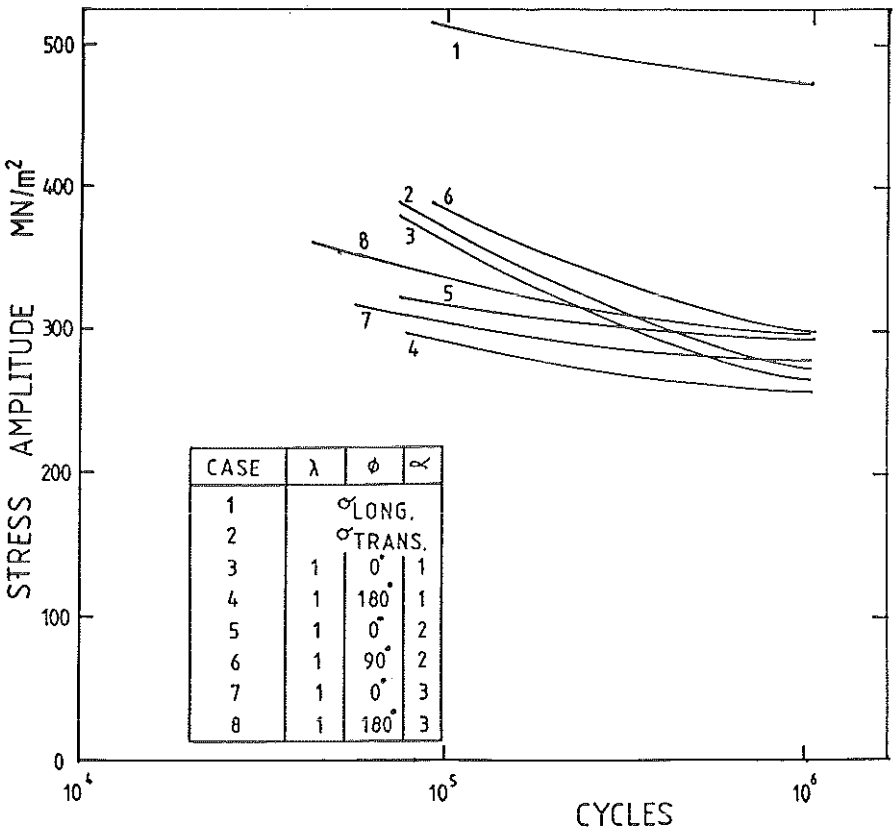

Fig 5 Test results – cases 1–8 from reference (7)

Table 3 shows the damaging shear stress amplitudes (*underlined*), as described in (7), occurring in each of the cases tested, considered as functions of the maximum applied principal stress amplitude. This table also shows the predicted and experimental fatigue limits as functions of the uniaxial longitudinal fatigue strength. The predicted value is based on the maximum shear stress criterion of failure and the experimental stress values are taken from Fig. 3 at 10^6 cycles. Data from (7) is shown for comparison and it can be seen for cases 4–8 that the experimental ratios σ_{1a}/σ_A are virtually the same, thus confirming the results of (7). As before the greatest difference between predicted and experimental results is about 15 per cent.

Series two tests

Figure 6 shows the results of tests to determine the effect of mean stress on longitudinal fatigue life. These results at 10^6 cycles, are found to agree closely

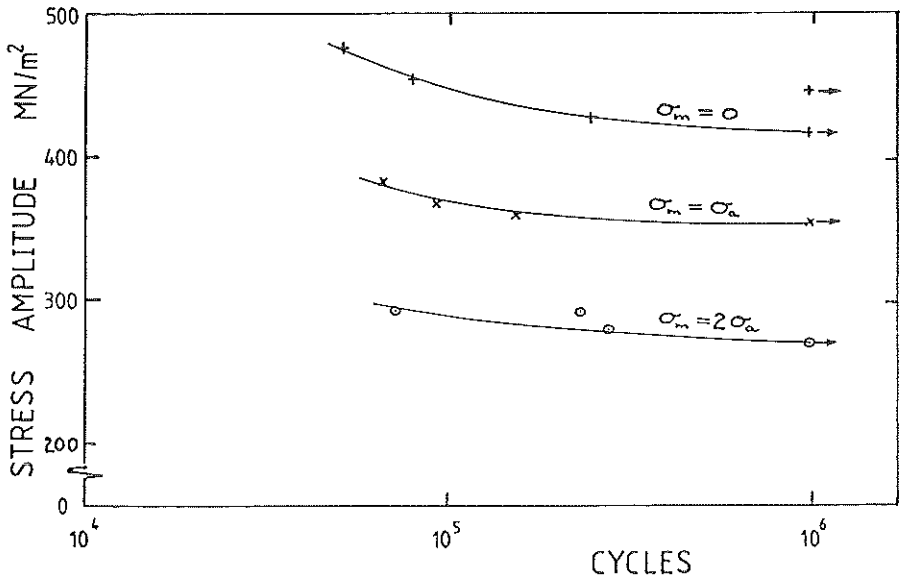

Fig 6 Test results – effect of longitudinal mean stress

with the Gerber parabolic relationship

$$\frac{\sigma_a}{\sigma_A} + \left(\frac{\sigma_m}{\sigma_T}\right)^2 = 1 \qquad (1)$$

Figure 7 shows the results of tests to determine the effect of mean stress on transverse fatigue life.

Series three tests

These tests investigated mean stress effects. It was pointed out earlier that the pressure applied in the pressure cell in order to produce a differential pressure across the wall thickness also produced a constant longitudinal tensile stress on the test specimen which could be offset by actuator load. This longitudinal tensile mean stress of 335 MN/m^2 on the specimen was not allowed for in the tests of (7) or the present series one tests. In a material of nominal tensile strength of 850 MN/m^2, this level of tensile mean stress, using equation (1), would produce a reduction of 15 per cent in alternating stress amplitude at 10^6 cycles.

For reasons of simplification of analysis, particularly in the cases where the biaxial stresses were not only out-of-phase but also at different frequencies, the analysis in (7) was conducted in terms of a shear stress criterion of failure which was found to be a reasonable basis for analysis, bearing in mind the limited amount of test data available.

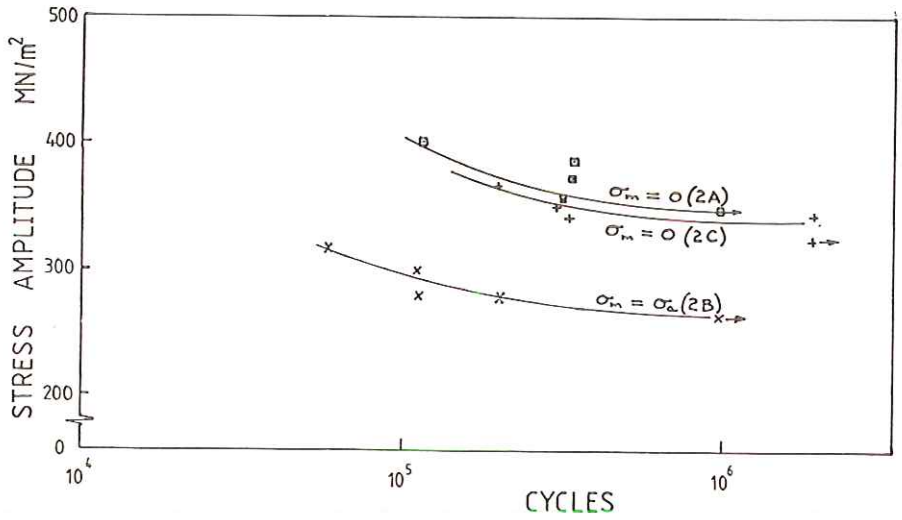

Fig 7 Test results – effects of transverse mean stress

It is known that fatigue failure is dependent not only on the shear stress amplitude on the plane of maximum range of shear stress but also on the secondary parameters of normal stress amplitude, mean normal stress and mean shear stress occurring on this plane, in that order of importance.

If we now consider the various possible combinations of mean stress and stress amplitude, both longitudinal and transverse in cases 1–4, where mean stress equals stress amplitude we can determine the critical planes of maximum range of shear stress and the stress conditions on these planes as shown in Table 4.

Case 1 tests were conducted without the pressure cell fitted and thus no mean longitudinal stress existed due to pressure. It is clear from Table 4 that the mean longitudinal stress present due to the pressure effect could affect which shear plane is critical in cases 2 and 3, depending on the degree of anisotropy in the test material, and also mean stress conditions on the critical shear plane in cases 2, 3, and 4.

Examination of Table 4 shows that it should be possible to determine the separate effects of the four effective stress parameters on the critical plane of maximum range of shear stress, here the *12* or *31* non-anisotropic shear planes, from cases 1A, 4A, 4B, and 4D. It is also seen that cases 1B, 1C, 2C, and 3B should give the same results.

It has been shown **(3)–(6)(8)** that the allowable amplitude of shear stress on the plane of maximum range of shear stress can be predicted from an equation of the form

$$\tau_a = C_1 - C_2\sigma_n^{1.5} - C_3\sigma_{nm}^2 - C_4\tau_m \qquad (2)$$

Table 4 Stresses on the plane of maximum range of shear stress for various combinations of alternating and mean longitudinal and transverse applied stresses

	Applied stresses (MN/m^2)								
	Longitudinal		*Transverse*		*Critical shear plane(s)*	$\frac{\tau_a}{\sigma_{1a}}$	$\frac{\sigma_n}{\sigma_{1a}}$	$\frac{\tau_m}{\sigma_{1a}}$	$\frac{\sigma_{nm}}{\sigma_{1a}}$
Case	*Amplitude*	*Mean*	*Amplitude*	*Mean*					
(1) Longitudinal stress									
1A	418				12, 31	0.5	0.5	–	–
1B	355	355			12, 31	0.5	0.5	0.5	0.5
1C	√			√	12	0.5	0.5	0.5	0.5
(2) Transverse stress									
2A			340		*23*	0.5	0.5	–	–
2B			262	262	*23*	0.5	0.5	0.5	0.5
2C		332	332		12	0.5	0.5	0.5	0.5
(3) $\lambda = 1$, $\varphi = 0$ degrees, $\alpha = 1$									
3A	√		√		*23*	0.5	0.5	–	–
3B	340	340	340		31	0.5	0.5	0.5	0.5
3C	√		√	√	*23*	0.5	0.5	0.5	0.5
3D	√	√	√	√	*23*	0.5	0.5	0.5	0.5
(4) $\lambda = 1$, $\varphi = 180$ degrees, $\alpha = 1$									
4A	278		278		12	1.0	0	–	–
4B	262	262	262		12	1.0	0	0.5	0.5
4C	230		230	230	12	1.0	0	0.5	0.5
4D	230	230	230	230	12	1.0	0	0	1.0

√ = To be tested.
Stress amplitude = Mean stress = σ_{1a}, at 10^6 cycles.
23 is the anisotropic (weakest) fatigue resistance plane.

where C_1, C_2, C_3, C_4 are material constants, namely

$$C_1 = t$$
$$C_2 = (t - b/2)/(b/2)^{1.5}$$
$$C_3 = (b/2)/(\sigma_T/2)^2$$

The available data in the literature (**9**) suggest that, provided the maximum shear stress in the cycle does not exceed that causing gross yielding, then the fatigue limit in pure torsion decreases only slightly with an increasing mean shear stress and, thus, C_4 is taken as zero at present. There is recent evidence (**12**) that this conclusion may have to be reconsidered, albeit that the effect of τ_m is certainly less than that of σ_n and σ_{nm}.

The value of C_2 has been found to agree with a large amount of combined bending and twisting fatigue test data (**3**) and also with the more limited test data available on thin wall cylinders under biaxial fatigue stress. When $C_1 = t$ is

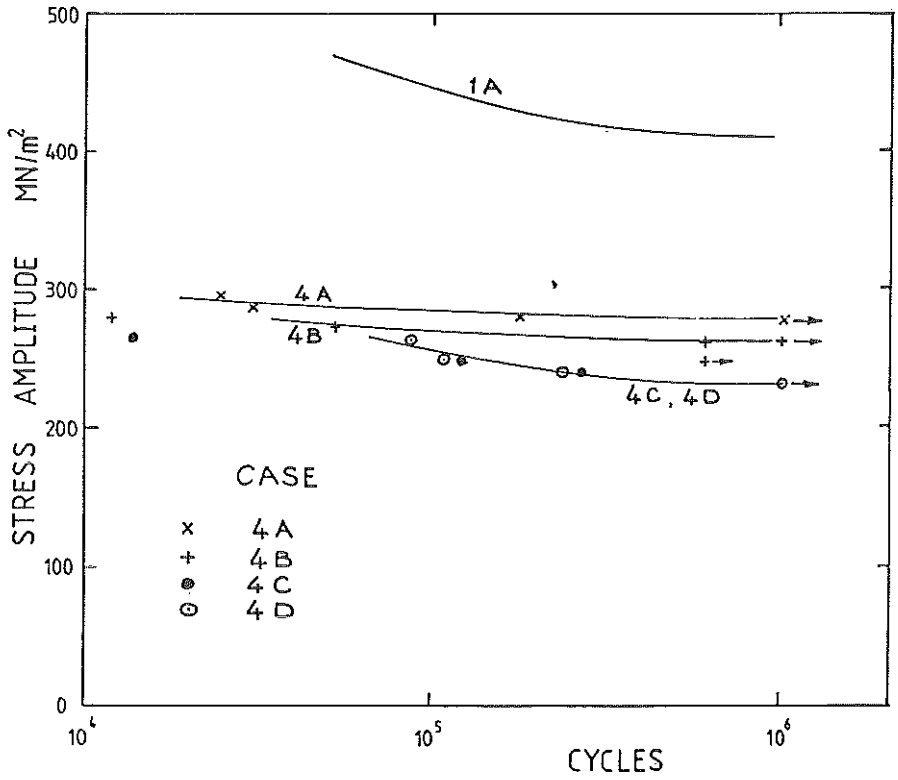

Fig 8 Test results – cases 1A, 4A, 4B, 4D

found from the reversed torsion test, it will include the effect of any anisotropy occurring in the material, whereas if C_1 is found from thin cylinder fatigue tests at $\lambda = 1$, $\phi = 180$ degrees, $\alpha = 1$ no anisotropic effect is included as the maximum range of shear stress does not act on the *23* anisotropic maximum shear stress plane.

C_3 is found (**8**) by applying the Gerber parabolic relationship (**10**) to stress conditions on the plane of maximum range of shear stress.

Extensive fatigue data is available for EN 25 (**11**) (a $2\frac{1}{2}$ per cent nickel–chromium–molybdenum steel) which is very similar to the EN 24T (a $1\frac{1}{2}$ per cent nickel–chromium–molybdenum steel) used in these tests. From this data $t = 284$ MN/m^2 from thin tubular specimens, $b = 479$ MN/m^2 from push pull tests, and $\sigma_T = 868$ MN/m^2. Hence

$C_1 = t = 284$ MN/m^2
$C_2 = (t - b/2)/(b/2)^{1.5} = 0.0118$
$C_3 = (b/2)/(\sigma_T/2)^2 = 0.00127$

giving, in equation (2)

$$\tau_a = 284 - 0.0118\sigma_n^{1.5} - 0.00127\sigma_{nm}^2 \quad (3)$$

Reference (**11**) also gives test data using solid specimens in rotating bending and reversed torsion from which $t = 301$ MN/m^2 and $b = 494$ MN/m^2 giving, in equation (2)

$$\tau_a = 301 - 0.0139\sigma_n^{1.5} - 0.00131\sigma_{nm}^2 \quad (4)$$

The results of test cases 1A, 4A, 4B, and 4D are shown in Fig. 8 and Table 5. From case 4A and equation (2)

$$\tau_a = 278 \text{ MN/m}^2 = C_1$$

From case 4D and equation (2)

$$\tau_a = 230 \text{ MN/m}^2 = C_1 - C_3(1.0 \times 230)^2$$

and, hence, $C_3 = 0.000907$.

From case 1A and equation (2)

$$\tau_a = (0.5 \times 418) \text{ MN/m}^2 = C_1 - C_2(0.5 \times 418)^{1.5}$$

and, hence, $C_2 = 0.0228$.

From case 4B and equation (2)

$$\tau_a = 262 \text{ MN/m}^2 = C_1 - C_3(0.5 \times 262)^2 - C_4(0.5 \times 262)$$

and, hence, C_4 is of the order of zero.

If the values of C_1 and C_2 found from cases 1A and 4B are accepted, and C_4 is taken to be zero, the value of C_3 can alternatively be found from the longitudinal mean stress tests shown in Fig. 6, values of 0.001 and 0.0014 being found.

Thus, from the test results, we obtain the general equation

$$\tau_a = 278 - 0.0228\sigma_n^{1.5} - 0.000907\sigma_{nm}^2 \text{ (MN/m}^2\text{)} \quad (5)$$

Table 5 Test results for cases 1–4 compared with results predicted from equation (5)

Case	σ_{1a} (MN/m^2 *at* 10^6 *cycles*)	$\frac{\tau_a}{\sigma_{1a}}$	$\frac{\sigma_n}{\sigma_{1a}}$	$\frac{\tau_m}{\sigma_{1a}}$	$\frac{\sigma_{nm}}{\sigma_{1a}}$	τ_a (*Test*) (MN/m^2)	τ_a (*Predicted*) (MN/m^2) *equation* (5)	$\frac{\tau_a \text{ (Predicted)}}{\tau_a \text{ (Test)}}$
1A	418	0.5	0.5	–	–	209	209	1.00
1B1	355	0.5	0.5	0.5	0.5	177	195	1.10
1B2	272	0.5	0.5	1.0	1.0	136	174	1.28
2A	340	0.5	0.5	–	–			
2B	262	0.5	0.5	0.5	0.5			
3B	340	0.5	0.5	0.5	0.5	170	201	1.18
4A	278	1.0	0	–	–	278	278	1.00
4B	262	1.0	0	0.5	0.5	262	262	1.00
4C	230	1.0	0	0.5	0.5	230	266	1.15
4D	230	1.0	0	0	1.0	230	230	1.00

This equation (5) is similar to the expressions already suggested in equations (3) and (4), with the exception that the test data show a greater effect of σ_n. The value of C_2 is particularly sensitive to the ratio t/b. For wrought steels t/b is found to range from 0.52 to 0.69, with an average value of 0.60 (**10**). When $t/b = 0.5$ then $C_2 = 0$. From the thin wall tube tests the equivalent value of t/b is found to be 278/418 = 0.67, an above average value and greater than the 0.58 value found from strain energy considerations. The value of $C_1 = t$ used here is also important since the effects of σ_n and σ_{nm} in the cases considered is only between 20 and 30 per cent of t.

It is of interest to compare predictions using equation (5) with the test results of cases 5–8 where the biaxial stresses are not only out-of-phase but also at different frequencies. Although these cases have not as yet been repeated with additional applied mean stresses, there are mean stress effects involved in the varying amplitude shear and normal stresses found to act on the plane of maximum range of shear stress. The fact that these stresses are not in-phase is ignored at this stage. For each cycle of σ_{1a} we obtain a number of cycles of τ_{12} and σ_{n12} of different amplitude depending on the value of the frequency ratio. Values of τ_{12} and σ_{n12} for cases 5 to 8 are shown in Table 6 taken from (**7**). For both shear and normal stresses only the cycles of greatest amplitude are considered to be damaging.

It is apparent from Table 5 that the effect of σ_{nm} found from Case 4D is low compared with that found in cases 1B and 3B. This anomaly may be due to the effect of material anisotropy. It is possible that the critical shear plane in cases 3B and 4D could be the anisotropic *23* plane. Further case 2 and 3 tests may help to clarify this matter.

If the σ_{nm} effect is defined using test data from case 1B rather than case 4D, until further investigation, then predictions using an expression of the form of

Table 6 Test results for cases 5–8 compared with results predicted from equation (5)

case	σ_{1a} $(MN/m^2$ *at* 10^6 *cycles)*	$\frac{\tau_a}{\sigma_{1a}}$	$\frac{\sigma_n}{\sigma_{1a}}$	τ_a *(Test)* (MN/m^2)	τ_a *(Predicted)* (MN/m^2) *equation* (5)	$\frac{\tau_a \text{ (Predicted)}}{\tau_a \text{ (Test)}}$
5	250	0 ± 0.88 0 ± 0.18	0 ± 0.88 0 ± 0.18	225	201	0.89
6	260	0 ± 0.78 0.28 ± 0.28	−0.12 ± 0.78 ±0.28 ± 0.28	208	210	1.01
7	230	0 ± 1.00 0 ± 0.26 0 ± 0.26	0 ± 0.76 0.38 ± 0.38 −0.38 ± 0.38	236	223	0.95
8	260	0 ± 0.76 0 ± 0.38 0 ± 0.38	0 ± 1.00 0 ± 0.26 0 ± 0.26	201	180	0.90

equation (5) are found to be within the order ±10 per cent of test results for cases 1–8.

Conclusions

(1) The maximum shear stress criterion of fatigue failure, modified for the effects of mean and alternating normal stresses acting on the plane of maximum range of shear stress, is a reasonable basis for long life fatigue predictions under complex stress situations such as out of phase biaxial stresses of different frequency including the effect of mean stress.
(2) The effect of mean normal stress acting on the plane of maximum range of shear stress can be predicted using a parabolic expression such as that suggested by Gerber.
(3) The effect of mean shear stress acting on the plane of maximum range of shear stress is small compared to the effect of normal stress.
(4) Material anisotropy is an important parameter when the maximum range of shear stress acts on the anisotropic (weakest) shear stress plane.

Acknowledgements

The author gratefully acknowledges the support of the Science and Engineering Research Council. Thanks are also due to Mr J. Edwards for conducting the tests.

References

(1) BROWN, M. W. and MILLER, K. J. (1973) A theory for fatigue failure under multiaxial stress–strain conditions, *Proc. Inst. mech. Engrs*, **187**, 745–755.
(2) GARUD, Y. S. (1981) Multiaxial fatigue: a survey of the state of the art, *J. Testing Evaluation*, **9**, 165–178.
(3) McDIARMID, D. L. (1972) *Failure criteria and cumulative damage in fatigue under multiaxial stress conditions*, PhD thesis, The City University, London.
(4) McDIARMID, D. L. (1973) A general criterion of fatigue failure under multiaxial stress, *Proceedings, Second International Conference on Pressure Vessel Technology*, American Society of Mechanical Engineers, New York, pp. 851–862.
(5) McDIARMID, D. L. (1977) A criterion of fatigue failure under out of phase multiaxial stresses, *Proceedings, Sixth Canadian Congress of Applied Mechanics*, Vancouver, Canada, pp. 245–246.
(6) McDIARMID, D. L. (1981) Fatigue under out of phase bending and torsion, *Aeronaut. J. Roy. Aeronaut. Soc.*, 118–122.
(7) McDIARMID, D. L. (1985) Fatigue under out of phase biaxial stresses of different frequencies, *ASTM STP 853*, ASTM, Philadelphia, PA, pp. 606–621.
(8) McDIARMID, D. L. (1985) The effects of mean stress and stress concentration on fatigue under combined bending and twisting, *Fatigue Fracture Engng Mater. Structures*, **8**, 1–12.
(9) SMITH, J. O. (1942) Effect of range of stress on fatigue strength. University of Illinois Engineering Experimental Station, Bulletin No. 334.
(10) FORREST, P. G. (1962) *Fatigue of metals*, Pergamon Press, London.
(11) MORRISON, J. L. M., CROSSLAND, B., and PARRY, J. S. C. (1960) Strength of thick cylinders subjected to repeated internal pressure, *Proc. Instn mech. Engrs*, **174**, 95–117.
(12) GRUBISIC, V. and SIMBURGER, A. (1976) *Fatigue testing and design*, Society of Environmental Engineers, London, pp. 27.1–27.8.